www.czasopisma.pan.pl PAN www.journals.pan.pl
POLSKA AKADEMIA NAUK

ACTA BIOLOGICA CRACOVIENSIA Series Botanica 57/2: 38–48, 2015
DOI: 10.1515/abcsb-2015-0022

NH_4^+-MEDIATED PROTEIN PHOSPHORYLATION IN RICE ROOTS

XIAO FENG ZHU[1#], WAN HUI CAI[2#], JIN HEE JUNG[3] AND YUAN HU XUAN[1*]

[1]*College of Plant Protection, Shenyang Agricultural University, Dongling Road 120, Shenyang, Liaoning, China 110866*
[2]*College of Pharmaceutical Sciences, Wenzhou Medical University, Wenzhou, Zhejiang, China 325035*
[3]*Department of Biotech R&D, Amicogen Inc, Jinju, South Korea 660751*

Received March 16, 2015; revision accepted September 10, 2015

NH_4^+ is an important N-source which regulates plant growth and development. However, the underlying mechanism of NH_4^+ uptake and its-mediated signaling is poorly understood. Here, we performed phosphoproteomic studies using the titanium dioxide (TiO_2)-mediated phosphopeptides collection method together with LC-MS analysis. The results indicated that phosphorylation levels of 23 and 43 peptides/proteins involved in diverse aspects, including metabolism, transport and signaling pathway, were decreased and increased respectively after NH_4^+ treatment in rice roots. Among 23 proteins detected, IDD10, a key transcription factor in ammonium signaling, was identified to reduce phosphorylation level of S313 residue. Further biochemical analysis using IDD10-GFP transgenic plants and immunoprecipitation assay confirmed that NH_4^+ supply reduces IDD10 phosphorylation level. Phosphorylation of ammonium transporter 1;1 (AMT1;1) was increased upon NH_4^+ treatment. Interestingly, phosphorylation of T446, a rice specific residue against *Arabidopsis* was identified. It was also established that phosphorylation of T452 is conserved with T460 of *Arabidopsis* AMT1;1. Yeast complementation assay with transformation of phosphomimic forms of AMT1;1 (T446/D and T452/D) into 31019b strain revealed that phosphorylation at T446 and T452 residues abolished AMT1;1 activity, while their plasma membrane localization was not changed. Our analyses show that many proteins were phosphorylated or dephosphorylated by NH_4^+ that may provide important evidence for studying ammonium uptake and its mediated signaling by which rice growth and development are regulated.

Key words: ammonium, phosphoproteomics, IDD10, AMT1;1, rice roots

INTRODUCTION

In higher plants, ammonium and nitrate are major sources of nitrogen for roots. NH_4^+ ions accumulate in the cells either by direct uptake from the rhizosphere via ammonium transporters (*AMTs*) or by reduction of NO_3^-. NH_4^+ is an energetic N-source because the reduction of nitrate to ammonium consumes 12–26% of photosynthesis products, but many plants exhibit a toxic symptom when its concentration is high (Bloom, 1997; Britto and Kronzucker, 2002; Noctor and Foyer, 1998). Paddy soil grown rice plants utilize NH_4^+ as major N-source due to poor aeration (Sasakawa and Yamamoto, 1978). NH_4^+ is taken up directly from the rhizosphere via plasma membrane located ammonium transporters (AMTs), which are later assimilated into the amino acid glutamate via the glutamine synthetase/glutamate synthase (GS/GOGAT) cycle. N-assimilation is also linked to carbon and respiratory metabolism by the demands of the GS/GOGAT cycle for reductants and 2-oxoglutarate (2-OG) as a carbon skeleton (Galvez et al., 1999).

Transcriptomics aimed at the collection and quantification of pools of differentially expressed transcripts, has been widely used in biological study. In *Arabidopsis*, a series of transcriptome analyses have demonstrated that N nutrient regulated expressions of global genes involved in diverse aspects including metabolic and developmental processes (Gutierrez et al., 2008; Patterson et al., 2010; Scheible et al., 2004; Wang et al., 2000). In rice, *AMT1;1* and *AMT1;2* are up-regulated in response to NH_4^+, whereas *AMT1;3* is up-regulated by nitrogen deprivation (Kumar et al., 2003; Sonoda et al., 2003). Further, NH_4^+ mediated induction of

*e-mail: yuanhu115@naver.com

#These authors contributed equally to this work.

PL ISSN 0001-5296

GS1;2 and *NADH-GOGAT1* in rice roots was identified (Tabuchi et al., 2007). Recently, the role of a key transcription factor IDD10 (Indeterminate domain 10) encoding a zinc finger protein in global regulation of ammonium-mediated gene expressions in rice roots was characterized (Xuan et al., 2013). Protein phosphorylation is one of the most important reversible modifications involved in many cellular processes such as metabolism, homeostasis, transcriptional and translational regulation, degradation of proteins, cellular signaling and communication, proliferation, differentiation and cell survival (Graves and Krebs, 1999). Previous studies have analyzed stimulus-induced protein phosphorylation patterns by sucrose, elicitor treatment, phytohormone and light (Benschop et al., 2007; Chen et al., 2010; Niittyla et al., 2007; Reiland et al., 2009; Tang et al., 2008). Global dynamic phosphorylation patterns regulated by re-supply of nitrate and ammonium to N starved *Arabidopsis* were identified and compared (Engelsberger and Schulze, 2012). *Arabidopsis* AMT1;1 phosphorylation at T460 is triggered by ammonium in a time- and concentration-dependent manner, and which in turn inhibits AMT1;1 activity (Lanquar et al., 2009).

Previous studies analyzed stimulus inducing enrichment ability of titanium dioxide (TiO_2) against phorphopeptides in different organisms including plants (Chen et al., 2010; Larsen et al., 2005; Thingholm et al., 2006). This method skips 2D gel and follows staining steps making easy collection of phosphopeptide from extracts. In this study, we used TiO_2 to collect phosphopeptide whose levels are modulated by ammonium in rice roots. 23 and 43 peptides were identified with their phosphorylation levels decreased or increased upon ammonium treatment, respectively. Interestingly, reduced IDD10 phosphorylation and increased AMT1;1 phosphorylation were identified. In addition, phosphorylation of T446 near T452 which is conserved with T460 of AtAMT1;1 was identified in OsAMT1;1. Immunoprecipitation and yeast complementation assays revealed that IDD10 and AMT1;1 phosphorylation may play important roles in alteration of protein activity. This work analyzes ammonium-mediated phosphoproteome, and provides information for further understanding of ammonium signaling pathway in rice.

MATERIALS AND METHODS

PLANT GROWTH

Oryza sativa Japonica rice cv Dongjin was used for the experiments. The following growth conditions were used to examine the effects of ammonium on gene expression and protein phosphorylation: germinated seeds were grown in tap water in a glasshouse for 14 days; the seedlings were grown for another 3 days in the N-free nutrient solution (Abiko et al., 2005); the seedlings were then transferred to a nutrient solution containing 0.5 mM $(NH_4)_2SO_4$ at pH 5.5; whole roots were harvested at 0, 1, 3 and 6 h following the provision of $(NH_4)_2SO_4$ (Xuan et al., 2013).

PHOSPHOPEPTIDE ENRICHMENT WITH TiO_2

Total protein was extracted from the plant roots. For this, 500 μg of total protein measured by a bicinchoninic acid assay, was solubilized in 7 M urea, 2 M thiourea, 2% CHAPS, 40 mM Trizma base, 50 mM DTT and 1% cocktail and 1% phosphatase inhibitor. Then the proteins were digested overnight by trypsin (1:50 wt/wt) at 37°C. Peptides were extracted and incubated for 15 min in 25 mM ammonium bicarbonate and 15 min in 5% formic acid. Samples were desalted on a C18 column according to the manufacturer's instructions and dried using a SpeedVac. The used phosphopeptide enrichment procedures were described (Larsen et al., 2005). TiO_2 beads were equilibrated prior to binding of phosphopeptide by aspirating/expelling 200 μl of 30 mg/ml 2,5-dihydroxybenzoic acid (DHB) in 80% acetonitrile and 0.1% TFA. Before binding, the trypsin-digested peptide lysate was adjusted to pH ≤ 1.9 by adding 1% TFA. Each peptide mixture was then added to a 2 ml reaction tube containing 10 mg of the TiO_2 beads and incubated batch-wise with end-over-end rotation for 30 min. After incubation, the beads were spun down at 500 g and briefly washed once with 80% acetonitrile, 0.1% TFA and once with 10% acetonitrile, 0.1% TFA. Finally, the bound peptides were eluted from the beads using 200 μl NH_4OH in 30% acetonitrile (pH > 10). The eluates were immediately neutralized in 5% TFA solvent and dried.

LC-MS/MS AND DATA PROCESSING

TiO_2 enriched phosphopeptides (4 μl) were submitted to on-line nanoflow liquid chromatography using the easy-nano LC system (Proxeon Biosystems, Odense, Denmark, now part of Thermo Fisher Scientific) with 10 cm capillary columns of an internal diameter of 75 μm filled with 3 μm Reprosil-Pur C18-A2 resin (Dr. Maisch GmbH, Ammerbuch-Entringen, Germany). The gradient consisted of 10–30% (v/v) CAN in 0.1% (v/v) formic acid at a flow rate of 200 nl/min for 45 min, 30–100% (v/v) CAN in 0.1% (v/v) formic acid at a flow rate of 200 nl/min for 1 min and 100% CAN in 0.1% formic acid at a flow rate of 200 nl/min for 10 min. The elution was electrosprayed through a Proxeon nanoelectrospray ion source by (electrospray ionization) ESI-MS/MS analysis on a Thermo Fisher LTQ Velos Pro

(Thermo Fisher Scientific, Bremen, Germany) using full ion scan mode over the m/z range 200–1800. Collision-induced dissociation (CID) was performed in the linear ion trap using a 4.0-Th isolation width and 35% normalized collision energy with helium as the collision gas. Five dependent MS/MS scans were performed on each ion using dynamic exclusion. Also, the precursor ion that had been selected for CID was dynamically excluded from further MS/MS analysis for 30s. The MS/MS spectra were processed using Proteome Discoverer (Version 1.3, Thermo Fisher Scientific, USA) and the database search was performed using Mascot search engine (Matrix Science Mascot 2.3) against a concatenated target-decoy approach.

The Swiss-Prot protein sequence database (release 54.5) was searched, with corresponding taxonomy selection for different samples. The search parameters were following: mass error tolerance for the precursor ions, 1 Da; mass error tolerance for the fragment ions, 0.8 Da; fixed modifications, carbamidomethylation (C); variable modifications, oxidation (M), phosphorylation (S, T, Y); number of missed cleavages, 1; significance threshold, $P < 0.05$; type of instrument, ESI-TRAP. Protein identifications were validated only if they satisfied the following 3 requirements: (a) their score was significant ($P < 0.05$) with cut-off criteria; (b) they were identified with one peptide with a score >15; (c) they were identified in at least two out of the three runs. Proteins identified by a set or subset of peptides used for identification of another protein were not taken into account.

RNA EXTRACTION AND QRT-PCR

Total cellular RNA was isolated from 20 of 17-day-old plant roots (Xuan et al., 2013) with TRIzol (Takara, Dalian, Liaoning, China) and subsequently 2 μg of total RNA was treated with RQ-RNase free DNase (Promega, Madison, WI, USA) to eliminate genomic DNA contamination. For cDNA synthesis, a GoScript Reverse Transcription kit was used following the manufacturer's instructions (Promega, Madison, WI, USA). qRT-PCR was performed in triplicate use of a SYBR green mix (Bio-rad). The reactions consisted of initial denaturation at 95°C for 3 min, followed by 40 cycles of denaturation for 15s, annealing for 20s at 60°C, and extension at 72°C for 20 s, followed by a final extension at 72°C for 10 min. The PCR products were quantified using an Illumina Research Quantity software Illumina Eco 3.0, (Illumina, San Diego, California, USA), and values were normalized against *Ubiquitin* levels from the same samples to analyze the ratio for each gene. Changes in gene expression were calculated via the *ΔΔCt* method (Han et al., 2006). The primers used for qRT-PCR are shown in Table S1.

PROTEIN EXTRACTION AND IMMUNOPRECIPITATION ASSAY

For total protein extraction, whole plant roots from 30 of 17-day-old seedlings (Xuan et al., 2013) were briefly ground into fine power in liquid nitrogen with moral and pestle, and then transferred to a 15 ml falcon tube. Further, a lysis buffer (100 ml of 5 mM Tris-HCl (pH 9.5), 5 mM EDTA, 4 M urea, 0.01% NaN_3) was added to a final tissue concentration of 1 mg/mL. The tissues were homogenized manually until no more bulks were visible. The homogenized samples were centrifuged at 15,000 g for 30 min at 4°C. The supernatant was collected and protein concentration was measured by Bradfold (Bio-Rad, Hercules, CA, USA) following the manufacturer's instruction. The supernatant was used for phosphoproteomic study.

Root tissues of the 20 plants overexpressing IDD10:GFP were harvested before and after ammonium treatment for 1 hour. The harvested tissues were ground in liquid nitrogen, homogenized in 2 ml of immunoprecipitation buffer (50 mM Tris-Cl at pH 7.5, 1 mM EDTA, 75 mM NaCl, 0.1% Triton X-100, 5% glycerol, 1mM phenylmethylsulphonyl fluoride, 1% protease inhibitor) and sonicated four times to break the nuclei. Centrifugation (15,000 g, 15 min at 4°C) was performed to collect the protein-containing supernatant, which was subsequently incubated with 1 μg of anti-GFP antibody (Abcam, USA) overnight at 4°C. Immune complexes were collected by incubating with Protein G Plus-Agarose (GE Healthcare) for 2 h at 4°C and washed three times with 1 ml of immunoprecipitation buffer. The immunoprecipitated proteins were eluted in the 2x loading buffer (Oh et al., 2012).

The eluted samples were then subjected to electrophoresis on 10% SDS-PAGE gel at 120 V. After the electrophoresis of the gel, the proteins were transferred to polyvinylidene fluoride membrane. Membranes were blocked with 5% bovine serum albumin in Tris-buffered saline containing 0.1% Tween 20 and incubated with the anti-GFP or anti-phospho (detect phosphorylation at T, S and Y residues) antibodies (Abcam, USA) for 2 hrs at 4°C. The proteins of interest were detected after incubation with horseradish peroxidase-conjugated secondary antibodies (Dako Cytomation, Glostrup, Denmark) and visualized with enhanced chemoluminiscence reagent ECL (GE Healthcare, Buckinghamshire, UK).

AMMONIUM UPTAKE DEFECTIVE STRAIN COMPLEMENTATION ASSAY

Ammonium uptake deficiency yeast strain 31019b (*Δmep1, Δmep2, Δmep3, ura3*) (Marini et al., 1997) was obtained from the Frommer lab (Carnegie insti-

tution for science). pDRf1-GFP GW vector harboring wild-type and mutant AMT1;1 (T446/D and T452/D) was transformed into yeast cells. Each transformant was plated in yeast nitrogen base (YNB) media containing 0.2 mM NH_4Cl or 1 mM arginine and yeast growth was monitored. The primers used for cloning the wild-type and mutant *AMT1;1* were listed in Table S1.

LOCALIZATION OF AMT1;1 IN YEAST

Wild-type and mutant AMT1;1 ORFs were cloned into the pDRf1-GFP GW vector (L. Q. Chen et al., 2010). The 31019b (*Δmep1, Δmep2, Δmep3, ura3*) yeast strain was transformed, and three independent colonies from each transformant were cultured in yeast nitrogen base (YNB) media containing 1 mM arginine. GFP fluorescence was detected under a confocal microscope (OLYMPUS).

RESULTS

IDENTIFICATION OF THE PHOSPHOPROTEINS RESPONDING TO NH_4^+

To determine phosphorylation changes upon NH_4^+ treatment, wild-type rice roots with or without NH_4^+ treatment for 1 hour were analyzed for three biological replicates. After trypsin digestion and TiO_2 enrichment, the phosphopeptides were identified by using the easy-nano LC system (Cong et al., 2014). The phosphopeptides that disappeared after ammonium treatment compared to the satate before the treatment were classified into a phosphorylation decreased group. In contrast, the phosphopeptides that were identified only after ammonium application were classified into a phosphorylation increased group. In total, we observed 23 peptides whose phosphorylations were decreased after ammonium treatment. Those proteins were diverse including auxin transporter, ethylene signaling transcription factor (AP2/ERF), protein phosphatase 2C (PP2C), potassium channel, trehalose-phosphate phosphatase and a key ammonium signaling transcription factor IDD10 (ZOS4-11 – C2H2 zinc finger protein) (Table 1). In contrast, there were 43 peptides whose phosphorylation levels were increased after ammonium supply. Those proteins include mitogen-activated protein kinase 4 (MAPK4), 14-3-3-like protein, auxin response factors, cytokinin dehydrogenase 8, ferredoxin-dependent glutamate synthase, pyruvate phosphate dikinase 2, AMT1;1 and potassium transporters (Table 2). These data indicate that ammonium triggers modulation of protein phosphorylation status involved in diverse aspects of phytohormone, metabolism, small molecule transport and cytoskeleton regulation.

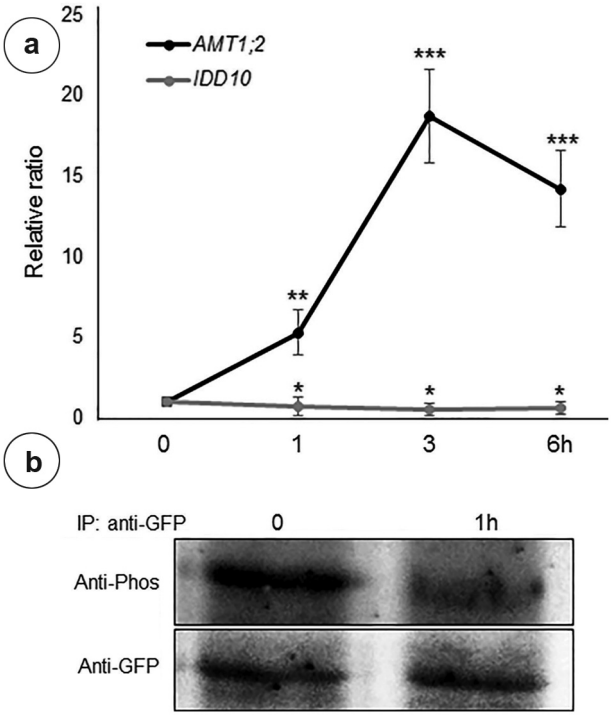

Fig. 1. NH_4^+-dependent transcriptional and post-translational changes of IDD10. Seventeen-day-old seedlings were transferred to nutrient solution containing 0.5 mM $(NH_4)_2SO_4$. Whole roots were sampled at 0, 1, 3 and 6 h after the addition of ammonium. (**a**) qRT-PCR was performed to determine the expression levels of AMT1;2 and IDD10. (**b**) Seventeen-day-old IDD10-GFP transgenic plants were transferred to nutrient solution containing 0.5 mM $(NH_4)_2SO_4$. whole roots were sampled at 0 and 1 h after NH_4^+ supply. GFP antibody was used for immuno-precipitation, and the levels of total IDD10 and phosphorylated IDD10 from the immune-precipitants were detected by GFP- and phospho- antibodies, respectively.

IDD10 PHOSPHORYLATION LEVEL WAS SIGNIFICANTLY DECREASED AFTER NH_4^+ TREATMENT

To confirm the data observed during the phosphoproteomic study, further immunoprecipitation assay was performed. Previously, we identified the role of a key transcription factor IDD10 in ammonium-mediated gene expressions in rice roots (Xuan et al., 2013). *IDD10* transcript was repressed, while *AMT1;2* was highly induced by NH_4^+ (Fig. 1a) (Xuan et al., 2013). Seventeen-day-old IDD10-GFP transgenic plants were transferred to 0.5 mM $(NH_4)_2SO_4$, and whole roots were sampled after 0 and 1 hour. Total soluble protein from IDD10-GFP plant roots was immunoprecipitated with GFP antibody, and the precipitants were immunoblotted with GFP and phospho antibodies, respectively. The results show

TABLE 1. Phosphorylation levels decreased upon NH_4^+ treatment.

No.	Description	Mr	pI	Phosphorylated Peptide	Ion Score	E-value	Ion precursor	Ion Charge
				Signaling				
1	BURP domain-containing protein 9	59621	6.12	K.FYLYNKGQAKDGDDQK.M	34	0.0053	1025.2848	2
2	Auxin transport protein BIG	560057	5.71	R.ELIAGSGALACLSK.F	22	0.027	735.5029	2
3	Putative B3 domain-containing protein	119710	9.55	K.DSSSKGNKIGNTR.S	32	0.014	722.4897	2
4	Zinc finger CCCH domain-containing protein 34	56909	6.04	K.SLADPLSLCSTSVK.A	26	0.016	779.7509	2
5	ZOS4-11 - C2H2 zinc finger protein	37682	5.38	R.LDHLLSPSGASAFRPPQPA FFLNAAAAAAATGQDFGDDA GNGQHSFLQAK.P	36	0.028	937.78	3
6	AP2/ERF and B3 domain-containing protein	41583	9.51	M.DSTSCLLDDASSGASTGKK.A	16	0.044	990.6337	2
7	Protein argonaute 7	118621	9.41	K.NEDNAGGGGGGLGTGGN GGGGGGGSANGR.R	20	0.024	789.6432	3
8	PHD finger protein ALFIN-LIKE 6	30185	5.47	MEGGGGGGGGGGGGGGGG GGGGAPYATR.T	19	0.028	1127.7755	2
9	Probable protein phosphatase 2C 9	44644	5.39	K.AESSDKACSDAAMLLTKLA LAR.R	20	0.026	833.5590	3
				Metabolism				
10	Probable glucuronosyltransferase	44708	8.88	MGSSTDHGGAGGRGK.K	30	0.0087	767.7444	2
11	Probable trehalose-phosphate phosphatase 9	40531	5.73	R.TGGVGGDSCK.K	26	0.039	509.0244	2
12	Photosystem I P700 chlorophyll a apoprotein A2	82622	6.63	K.GALDARGSKLMPDK.K	25	0.026	777.5374	2
13	Putative 12-oxophytodienoate reductase 13	42208	5.24	R.GMFMVGGGYDRDAGNMA VASGYADMVVFGR.L	22	0.037	1103.4255	3
				Transport				
14	Probable protein transport Sec1b	75081	7.59	R.APKGTDPMTTPKFDMVPK.W	23	0.023	1068.7507	2
15	Two pore potassium channel c	50025	9.12	R.SRTAPAMAPLNAAAIAAAAA SGDSR.N	16	0.035	829.7567	3
				Others				
16	Formin-like protein 5	177326	6.58	R.ASAPPPPPPPSTR.L	26	0.022	451.5818	3
17	Putative glycine-rich cell wall structural protein 1	13830	9.52	K.YNGGESGGGGGGGGGG GGGNGSGSGSGYGYNYGK.G	21	0.041	1038.6849	3
18	Telomerase reverse transcriptase	146935	9.50	K.QTGSSTSAEEQK.Q	18	0.048	666.5851	2
19	Cyclin-SDS-like	52645	4.99	R.FLTRGYVKGSR.N	21	0.03	683.0961	2
20	Putative cyclin-F1-2	39696	5.55	R.ASMIAFMGEFSRK.N	25	0.015	794.2405	2
21	Probable nucleoredoxin 3	54277	6.72	R.EEYHLIFTNSNRK.T	25	0.031	577.9264	3
22	Pleiotropic drug resistance protein 6	162489	8.23	R.LTTGELLVGSAR.V	20	0.029	689.1671	2
23	ATP-dependent zinc metalloprotease FTSH 8	90246	7.16	R.ARGRGGFSGSNDER.E	19	0.037	813.0004	2

that phosphorylation of IDD10 was significantly decreased after ammonium supply compared with the similar IDD10 protein levels, suggesting that ammonium treatment specifically affects phosphorylation of IDD protein rather than the total protein expression (Fig. 1b).

TABLE 2. Phosphorylation levels increased by NH_4^+ supply.

No.	Description	Mr	pI	Phosphorylated Peptide	Ion Score	E-value	Ion precursor	Ion Charge
				Signaling				
1	Probable protein phosphatase 2C 19	72048	4.65	K.QRSAMGNSLPVESK.F	23	0.0450	800.4395	2
2	Mitogen-activated protein kinase 4	42673	6.86	R.GAYGIVCSSINRATNEK.V	25	0.0490	640.5626	3
3	14-3-3-like protein GF14-D	29358	4.83	K.QAFDEAISELDSLGEESY K.D	26	0.0055	1146.3535	2
4	Auxin response factor 21	124323	6.30	M.ASSGGGGGGGEEGEGR GATK.V	24	0.0480	919.7477	2
5	Auxin response factor 24	92877	6.31	K.MNPGALNSRSEDSR.S	25	0.0460	807.6729	2
6	Transcription initiation factor TFIID subunit 1	205459	5.48	R.NMSISASLVSDK.R	23	0.0180	746.3921	2
7	Calmodulin-like protein 5	18525	4.12	K.DQDGLISAAELR.H	27	0.0250	684.5238	2
8	Zinc finger CCCH domain-containing protein 16	78632	8.85	MSTAAADPAAAADAAVTR.K	22	0.0200	581.1310	3
9	Zinc finger CCCH domain-containing protein 55	106032	8.76	K.IDIYMSYSREK.L	21	0.0410	790.6273	2
10	Homeobox-leucine zipper protein ROC6	92575	5.75	R.SGSDNLDGASGDELDPD NSNPRK.K	18	0.0430	867.4716	3
11	Homeobox-leucine zipper protein ROC4	87671	5.59	K.MVTAAHGGVGGGGGGG RAK.A	15	0.0370	839.0505	2
12	Nucleolar complex protein 2 homolog	87097	6.84	K.ETVSELMITK.Q	27	0.0240	623.5174	2
13	23.6 kDa heat shock protein, mitochondrial	23805	7.74	R.ALFSSAGADAAATTGGC APAK.G	23	0.0200	1028.4167	2
14	Dehydration-responsive element-binding protein 2D	27957	5.08	MAAGEGDVGMEVETK.A	20	0.0220	818.6985	2
				Metabolism				
15	Ferredoxin-dependent glutamate synthase, chloroplastic	176359	6.42	R.TNTGVGMVFLPQDENS MEEAK.A	27	0.0380	792.6119	3
16	Putative diaminopimelate epimerase, chloroplastic	38564	6.22	R.FIAELENLQGTHSFK.I	27	0.0230	907.7107	2
17	Pyruvate phosphate dikinase 2	97232	5.42	R.GGMTSHAAVVAR.G	21	0.0490	619.1409	2
18	1,2-dihydroxy-3-keto-5-methylthiopentene dioxygenase 1	23855	5.07	K.TEVIEAWYMDDSEEDQR.L	35	0.0013	737.5872	3
19	Probable indole-3-acetic acid-amido synthetase GH3.7	69889	5.32	R.VPVSGYEDVKPYVDR.V	29	0.0060	942.2312	2
20	Probable histone acetyltransferase HAC-like 2	165606	8.20	K.EVIMTSLLSGK.I	26	0.0270	629.9850	2
21	40S ribosomal protein S8	24928	10.41	R.LDTGNYSWGSEAVTR.K	24	0.0280	967.6493	2
22	Ferredoxin--NADP reductase, embryo isozyme, chloroplastic	42130	8.85	M.ASALGAQASVAAPIGAG GYGRSSSSK.G	23	0.0190	934.6967	3
23	DEAD-box ATP-dependent RNA helicase 32	87286	9.16	R.NEEMDAGSENSGSESD R.D	23	0.0300	637.5721	3
24	Probable RNA-dependent RNA polymerase 2	127928	7.33	R.MGQLFSSSR.Q	20	0.0490	546.0216	2
25	Ent-sandaracopimara-8(14),15-diene synthase	92783	5.63	R.ALTDSGNTSPESIEAAK.E	20	0.0420	926.3646	2

TABLE 2. *Cont.*

				Metabolism *cont.*				
26	Probable indole-3-acetic acid-amido synthetase GH3.5	65738	5.42	R.RSLVLSINIDKNTEK.D	20	0.0360	604.0341	3
27	Cytokinin dehydrogenase 8	57981	5.98	R.VRMEEESLRSR.G	29	0.0420	496.4200	3
28	Zeaxanthin epoxidase, chloroplastic	72210	8.01	K.FDTFTPAAER.G	27	0.0390	617.4861	2
				Transport				
29	Ammonium transporter1-1	65430	5.78	L.RISAEDETSGMDLTRHG GFAYVYHDEDEHDK.S	37	0.0370	873.4000	3
30	Probable potassium transporter 14	95322	5.99	K.EDYISFQQLLIESLEK.F	26	0.0430	1058.5699	2
31	Potassium transporter 1	88705	8.89	R.HDSLFGDAEK.V	30	0.0028	599.9489	2
32	Probable anion transporter 5, chloroplastic	50153	6.40	R.ASPGEGGGGGGGGGGG GGLAGALEK.R	18	0.0330	655.4515	3
33	Inorganic phosphate transporter 1-2	58146	8.85	M.AGSQLNVLVK.L	52	0.0004	554.9319	2
34	Magnesium transporter MRS2-E	46543	5.06	R.SLEKEAYPALDK.L	33	0.0370	722.6066	2
35	Calcium-transporting ATPase 3, plasma membrane-type	113511	8.09	K.HTLVTNLR.G	20	0.0310	517.1622	2
36	Probable calcium-transporting ATPase 6, plasma membrane-type	113465	5.93	R.MHGGINGISR.K	23	0.0390	569.5954	2
				Others				
37	Tubulin beta-8 chain	50229	4.77	R.INVYFNEASGGRHVPRA VLMDLEPGTMDSLR.S	23	0.0440	1207.8286	3
38	Cellulose synthase-like protein	133673	8.13	R.HSLGSSTATLQVSPVR.R	15	0.0490	653.5317	2
39	Formin-like protein 14	90734	8.55	K.KASSIDMMKLSR.D	39	0.0100	779.6597	2
40	CASP-like protein	24765	8.44	MSGSDTSGSVHVDEHGH GK.A	25	0.0290	1042.2939	2
41	4-coumarate--CoA ligase-like 2	63688	6.52	K.IIITASAQSAFLLARVSNS SK.N	21	0.0290	779.6672	3
42	Endoribonuclease Dicer homolog 1	212065	6.23	K.DLAGMVVTAAHSGK.R	17	0.0310	766.7453	2
43	Golgin-84	79370	5.27	K.SLDSWKK.K	16	0.034	943.4867	1

AMT1;1 PHOSPHORYLATION AT T446 AND T452 RESIDUES AFFECTS ITS AMMONIUM TRANSPORT ACTIVITY

Environmental NH_4^+ ions are taken up into the cells via ammonium transporters (AMTS). AMT1;1 phosphorylation at two threonine residues were identified in our analyses (Table 2). In *Arabidopsis*, AMT1;1 is rapidly phosphorylated at T460 which in turn abolishes AMT1;1 function (Lanquar et al., 2009). To analyze the position of rice AMT1;1 phosphorylated residues, AtAMT1;1 and OsAMT1;1 sequences were aligned (Fig. 2). The results show that T452 of OsAMT1;1 is conserved with T460 of AtAMT1;1, while T452 is specific to OsAMT1;1 compared to AtAMT1;1 (Fig. 2). To test phosphorylation effects on AMT1;1 ammonium transport activity, wild-type and phosphomimic forms of AMT1;1 (T446/D and T452/D) were transformed into yeast strain 31019b (*Δmep1, Δmep2, Δmep3, ura3*) which is defective in ammonium uptake (Marini et al., 1997). For construction, ORFs of wild-type and mutant *AMT1;1* were C-terminally fused to *GFP* coding region via gateway cloning system into pDRf1 GW vector. Yeast cell growth was monitored in the media containing 0.2 mM NH_4Cl and 1 mM arginine. The data shown in Figure 3 suggest that wild-type AMT1;1 can transport ammonium while two phos-

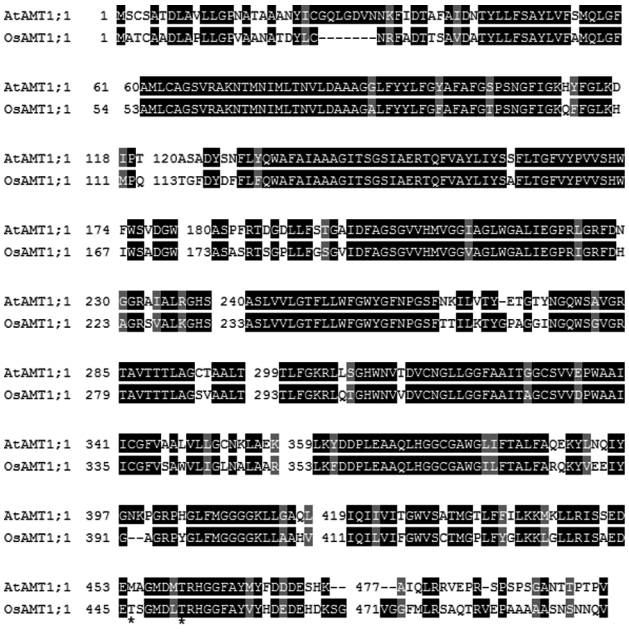

Fig. 2. Sequence alignment of AtATM1;1 and OsAMT1;1. Identical and similar amino acids are shown in black and gray boxes, respectively. Asterisks under the residues indicate the position of phosphorylated threonine.

phomimic forms of AMT1;1 (T446/D and T452/D) fail to transport ammonium into yeast cells. Further, AMT1;1 sub-cellular localization was examined in yeast cells. Yeast cells expressing wild-type and mutant forms of AMT1;1 were cultured in the medium containing 1 mM arginine and their localization was observed via a confocal microscopy. Wild-type and mutant forms of AMT1;1 are all located at the plasma membrane in yeast cells (Fig. 4). To sum up, these data indicated that phosphorylation at T446 and T452 at AMT1;1 did not change their sub-cellular targeting but abolished AMT1;1 ammonium transport activity.

DISCUSSION

NH_4^+ has long been thought to be the source of amino acid metabolism, and it was not considered as a signal molecule. However, researchers recently found that NH_4^+ itself regulates gene expressions without assimilation by supply of MSX, a glutamine synthetase inhibitor (Patterson et al., 2010). In *Arabidopsis*, ammonium triggers lateral root branching in an AMT1;3-dependent manner (Lima et al., 2010). Those findings implied that ammonium may act as a signal molecule and play an important role in plant growth and development. In rice, ammonium-mediated transcriptome and IDD10 regulation in ammonium-mediated gene expressions and primary root growth were analyzed (Xuan et al., 2013). Furthermore, AtAMT1;1 phosphorylation at its cytosolic tail T460 revealed an ammonium-dependent inhibitory mechanism of ammonium transporter (Lanquar et al., 2009).

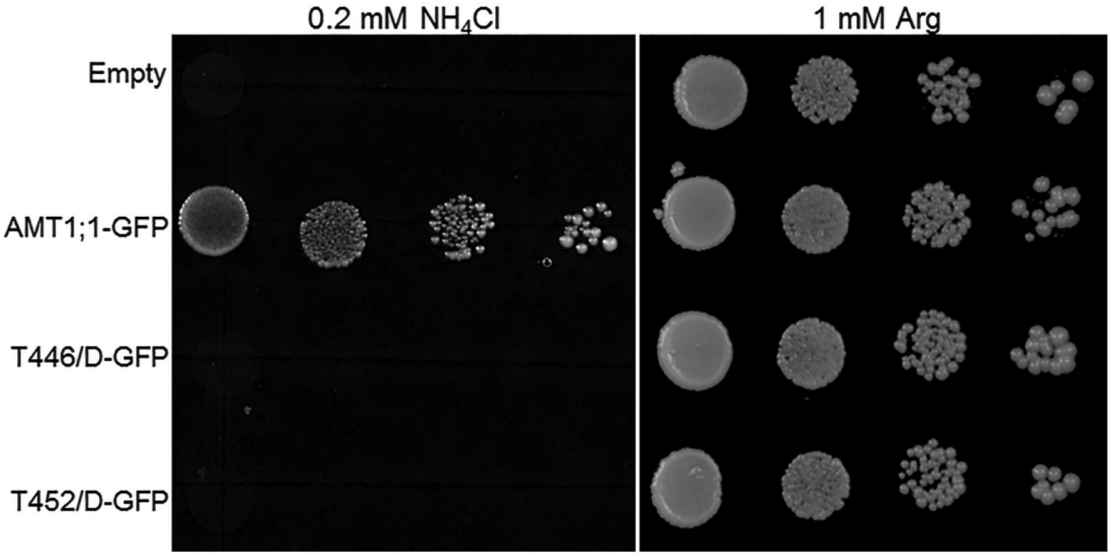

Fig. 3. Functional analysis of phosphomimic ATM1;1 proteins by complementation of an NH_4 uptake defective yeast strain 31019b (*Δmep1, Δmep2, Δmep3, ura3*). Yeast cells were transformed with wild-type and two mutant AMT1;1 or empty vector pDRf1-GFP and tested for growth complementation on YNB plates supplemented with 0.2 mM NH_4Cl or 1 mM arginine (Arg). Empty (pDRf1-GFP) vector and AMT1;1-GFP were used as the negative and positive controls, respectively. Yeast cells were grown at 30°C for 3 days.

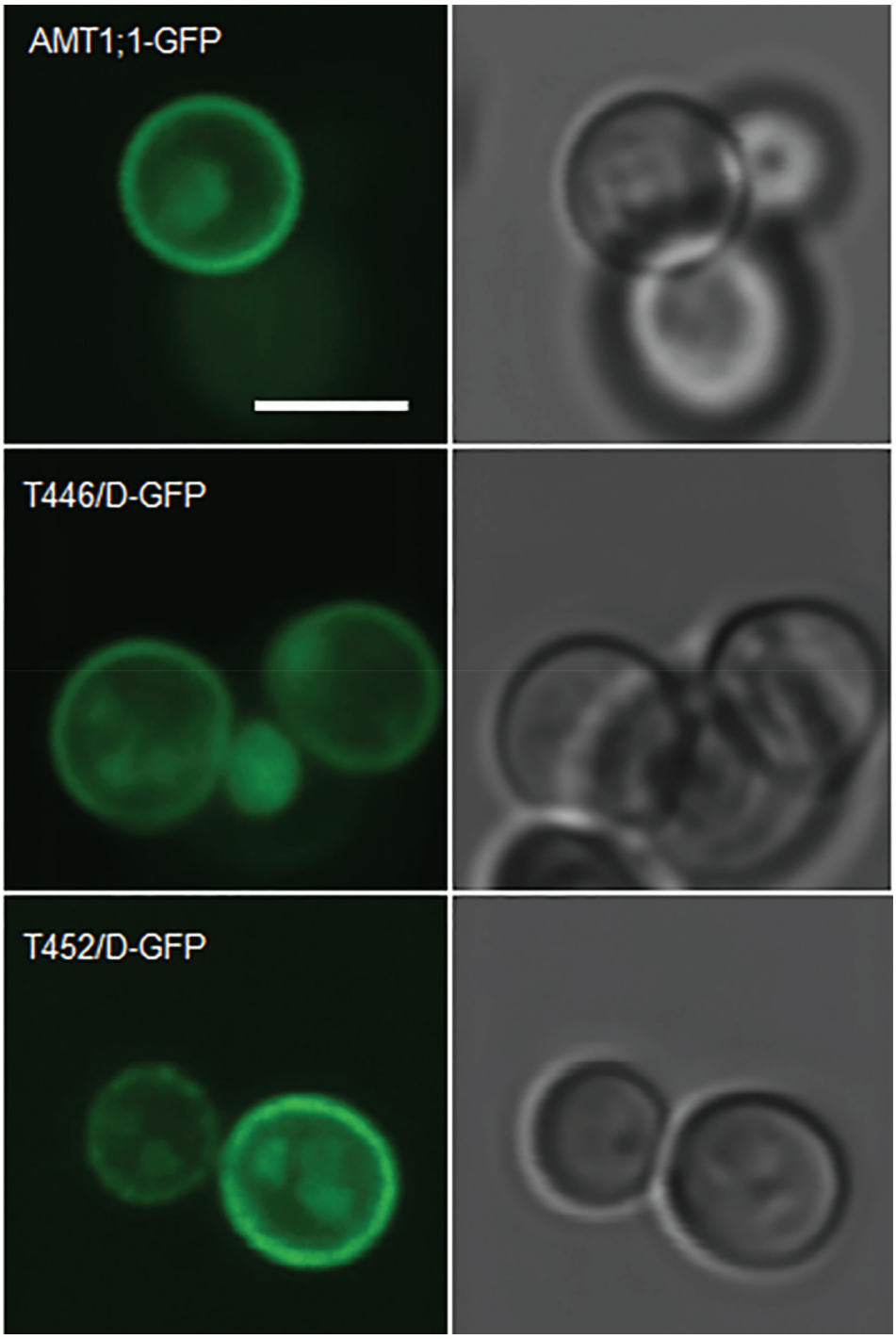

Fig. 4. Localization of wild-type and mutant AMT1;1 proteins in yeast. WT and mutant AMT1;1-GFP fusion proteins were expressed in the 31019b yeast strain. After growth on minimal medium with ammonium as the sole nitrogen source, cells were analyzed by confocal microscopy. (Left) GFP fluorescence and (Right) bright field images of AMT1;1-GFP, T446/D and T452/D. Scale bar =10 μm.

Our phosphoproteomic study in rice plant roots against NH_4^+ response identified many phosphorylated proteins involved in diverse aspects of signaling pathway. Modifications of auxin transporter, indole-3-acetic acid-amido synthetase GH3.5, auxin response factor 21 and 24 were identified. Effects of

ammonium on auxin-mediated lateral root emergence has been reported in *Arabidopsis* (Li et al., 2011). Cytokinin dehydrogenase 8 and zeaxanthin epoxidase are involved in cytokinin catabolism and biosynthesis, respectively, their phosphorylation was triggered by ammonium (Table 2). Ammonium-dependent transcriptome study also showed that cytokinin dehydrogenase gene expression was induced by ammonium (Xuan et al., 2013). Besides phytohormone signaling pathway, N- (ferredoxin-dependent glutamate synthase) and C- (trehalose-phosphate phosphatase and pyruvate phosphate dikinase 2) metabolism related protein phosphorylation was identified, indicating diverse regulation of ammonium in C- and N- metabolic proteins. Moreover, phosphorylation of the transporters including ammonium, potassium, phosphate and magnesium as wells as cytoskeleton related proteins, formin-like protein and tubulin was altered (Table 1 and 2). More interestingly, phosphorylation level of IDD10, an ammonium signaling key transcription factor, was reduced by ammonium (Fig. 1b). IDD10 was reported to directly bind to the specific *cis*-elements and activate transcription of genes harboring the IDD10-binding motif in their promoter and introns in an ammonium-dependent manner (Xuan et al., 2013). Expression of *AMT1;2*, a key ammonium transporter, was directly regulated by IDD10, but surprisingly *IDD10* transcript was slightly repressed by ammonium (Fig. 1a). Here, we observed that S313 located at the activation domain of IDD10 was phosphorylated. It was also confirmed that using IDD10-GFP transgenic plants and immunoprecipitation assay, reduced phosphorylation of IDD10 after ammonium-stimuli (Fig. 1b). These data imply that ammonium signaling may trigger repression of IDD10 phosphorylation to increase its transcriptional activity. Further mutagenesis and transcriptional assays are required to verify the role of phosphorylation at IDD10 S313. Ammonium transporter regulation by phosphorylation was reported in *Arabidopsis*. In our analyses, T452 at OsAMT1;1 which is conserved with T460 of AtAMT1;1 was also identified, indicating that similar regulatory mechanism occurred in *Arabidopsis* and rice. In addition, T446 which is located near T452 was also modulated by its ammonium-dependent phosphorylation. Complementation assay with rescue ammonium uptake defective strain 31019b indicated that phosphorylation of both T446 and T452 abolish AMT1;1 activity (Fig. 4). Further studies will focus on understanding of the molecular mechanisms of phosphorylation events in AMT1;1, which is important to explore the ammonium signaling perception and transduction pathways, especially involved in how ammonium transporters are regulated and how they transduce signaling in plants.

CONCLUSIONS

We analyzed ammonium dependent protein phosphorylation in rice which provided some information about ammonium-mediated proteome regulations, and identified some evidence important for understanding of regulatory mechanism of IDD10 and AMT1;1, two important proteins in ammonium signaling pathway.

AUTHOR'S CONTRIBUTION

XFZ, WHC and YHX designed the research; XFZ, WHC and JHJ performed the research; XFZ,WHC, JHJ and YHX analyzed the data; XFZ, WHC and YHX wrote the paper. All the authors read and approved the final manuscript, and declare that there are no conflicts of interest.

ACKNOWLEDGEMENTS

This work was supported by the startup funding from SAU to XFZ and YHX.

REFERENCES

Abiko T, Obara M, Ushioda A, Hayakawa T, Hodges M, and YAMAYA T. 2005. Localization of NAD-isocitrate dehydrogenase and glutamate dehydrogenase in rice roots: candidates for providing carbon skeletons to NADH-glutamate synthase. *Plant Cell Physiology* 46: 1724–1734.

Benschop JJ, Mohammed S, O'Flaherty M, Heck AJ, Slijper M, and Menke FL. 2007. Quantitative phosphoproteomics of early elicitor signaling in *Arabidopsis*. *Molecular Cell Proteomics* 6: 1198–1214.

Bloom AJ. 1997. Nitrogen as a limiting factor: crop acquisition of ammonium and nitrate. In: *Ecology in Agriculture* (ed. L.E. Jackson). Academic Press, San Diego, CA, USA. pp. 145–172.

Britto DT, and Kronzucker HJ. 2002. NH_4^+ toxicity in higher plants: a critical review. *Journal of Plant Physiology* 159: 567–584.

Chen LQ, Hou BH, Lalonde S, Takanaga H, Hattung ML, Qu XQ, Guo WJ, Kim JG, Underwood W, Chaudhuri B, Chermak D, Antony G, White FF, Somerville SC, Mudgett MB, and Frommer WB. 2010. Sugar transporters for intercellular exchange and nutrition of pathogens. *Nature* 468: 527–532.

Chen Y, Hoehenwarter W, and Weckwerth W. 2010. Comparative analysis of phytohormone-responsive phosphoproteins in *Arabidopsis* thaliana using TiO_2-phosphopeptide enrichment and mass accuracy precursor alignment. *Plant Journal* 63: 1–17.

Cong W, Shen J, Xuan Y, Zhu X, Ni M, Zhu Z, Hong G, Lu X, and Jin L. 2014. A simple, rapid and low-cost staining method for gel-electrophoresis separated phosphoproteins via the fluorescent purpurin dye. *Analyst* 139: 6104–6108.

Engelsberger WR, and Schulze WX. 2012. Nitrate and ammonium lead to distinct global dynamic phosphorylation patterns when resupplied to nitrogen-starved *Arabidopsis* seedlings. *Plant Journal* 69: 978–995.

Galvez S, Lancien M, and Hodges M. 1999. Are isocitrate dehydrogenases and 2-oxoglutarate involved in the regulation of glutamate synthesis? *Trends in Plant Science* 4: 484–490.

Graves JD, and Krebs EG. 1999. Protein phosphorylation and signal transduction. *Pharmacology and Therapeutics* 82: 111–121.

Gutierrez RA, Stokes TL, Thum K, Xu X, Obertello M, Katari MS, Tanurdzic M, Dean A, Nero DC, McClung CR, and Coruzzi GM. 2008. Systems approach identifies an organic nitrogen-responsive gene network that is regulated by the master clock control gene CCA1. *Proceeding National Academy of Science U.S.A.* 105: 4939–4944.

Han MJ, Jung KH, Yi G, Lee DY, and An G. 2006. Rice Immature Pollen 1 (RIP1) is a regulator of late pollen development. *Plant Cell Physiology* 47: 1457–1472.

Kumar A, Silim SN, Okamoto M, Siddiqi MY, and Glass AD. 2003. Differential expression of three members of the AMT1 gene family encoding putative high-affinity NH_4^+ transporters in roots of *Oryza sativa* subspecies indica. *Plant Cell Environment* 26: 907–914.

Lanquar V, Loque D, Hormann F, Yuan L, Bohner A, Engelsberger WR, Lalonde S, Schulze WX, von Wiren N, and Frommer WB. 2009. Feedback inhibition of ammonium uptake by a phospho-dependent allosteric mechanism in *Arabidopsis*. *Plant Cell* 21: 3610–3622.

Larsen MR, Thigholm TE, Jensen ON, Roepstorff P, and Jorgensen TJ. 2005. Highly selective enrichment of phosphorylated peptides from peptide mixtures using titanium dioxide microcolumns. *Molecular Cell Proteomics* 4: 873–886.

Li B, Li Q, Su Y, Chen H, Xiong L, Mi G, Kronzucker HJ, and Shi W. 2011. Shoot-supplied ammonium targets the root auxin influx carrier AUX1 and inhibits lateral root emergence in *Arabidopsis*. *Plant Cell Environment* 34: 933–946.

Lima JE, Kojima S, Takahashi H, and von Wiren N. 2010. Ammonium triggers lateral root branching in *Arabidopsis* in an AMMONIUM TRANSPORTER1;3-dependent manner. *Plant Cell* 22: 3621–3633.

Marini AM, Soussi-Boudekou S, Vissers S, and Andre B. 1997. A family of ammonium transporters in *Saccharomyces cerevisiae*. *Moleclular Cell Biology* 17(8): 4282–4293.

Niittyla T, Fuglsang AT, Palmgren MG, Frommer WB, and Schulze WX. 2007. Temporal analysis of sucrose-induced phosphorylation changes in plasma membrane proteins of *Arabidopsis*. *Molecular Cell Proteomics* 6: 1711–1726.

Noctor G, and Foyer CH. 1998. A re-evaluation of the ATP : NADPH budget during C3 photosynthesis: a contribution from nitrate assimilation and its associated respiratory activity? *Journal of Experimental Botany* 49: 1895–1908.

Oh E, Zhu JY, and Wang ZY. 2012. Interaction between BZR1 and PIF4 integrates brassinosteroid and environmental responses. *Nature Cell Biology* 14: 802–809.

Patterson K, Cakmak T, Cooper A, Lager I, Rasmusson AG, and Escobar MA. 2010. Distinct signalling pathways and transcriptome response signatures differentiate ammonium- and nitrate-supplied plants. *Plant Cell Environment* 33: 1486–1501.

Reiland S, Messerli G, Baerenfaller K, Gerrits B, Endler A, Grossmann J, Gruissem W, and Baginsky S. 2009. Large-scale *Arabidopsis* phosphoproteome profiling reveals novel chloroplast kinase substrates and phosphorylation networks. *Plant Physiology* 150: 889–903.

Sasakawa H, and Yamamoto Y. 1978. Comparison of the uptake of nitrate and ammonium by rice seedlings: influences of light, temperature, oxygen concentration, exogenous sucrose, and metabolic inhibitors. *Plant Physiology* 62: 665–669.

Scheible WR, Morcuende R, Czechowski T, Fritz C, Osuna D, Palacious-Rojas N, Schindelasch D, Thimm O, Udvardi MK, and Stitt M. 2004. Genome-wide reprogramming of primary and secondary metabolism, protein synthesis, cellular growth processes, and the regulatory infrastructure of *Arabidopsis* in response to nitrogen. *Plant Physiology* 136: 2483–2499.

Sonoda Y, Ikeda A, Saiki S, von Wiren N, Yamaya T, and Yamaguchi J. 2003. Distinct expression and function of three ammonium transporter genes (OsAMT1;1-1;3) in rice. *Plant Cell Physiology* 44: 726–734.

Tabuchi M, Abiko T, and Yamaya T. 2007. Assimilation of ammonium ions and reutilization of nitrogen in rice (*Oryza sativa* L.). Journal of Experimental Botany 58: 2319–2327.

Tang W, Deng Z, Oses-Prieto JA, Suzuki N, Zhu S, Zhang X, Burlingame AL, and Wang ZY. 2008. Proteomics studies of brassinosteroid signal transduction using prefractionation and two-dimensional DIGE. *Molecular Cell Proteomics* 7: 728–738.

Thingholm TE, Jorgensen TJ, Jensen ON, and Larsen MR. 2006. Highly selective enrichment of phosphorylated peptides using titanium dioxide. *Nature Protocol* 1: 1929–1935.

Wang R, Guegler K, Labrie ST, and Crawford NM. 2000. Genomic analysis of a nutrient response in *Arabidopsis* reveals diverse expression patterns and novel metabolic and potential regulatory genes induced by nitrate. *Plant Cell* 12: 1491–1509.

Xuan YH, Priatama RA, Huang J, Je BI, Liu JM, Park SJ, Piao HL, Son DY, Lee JJ, Park SH, Jung KH, Kim TH, and Han CD. 2013. Indeterminate domain 10 regulates ammonium-mediated gene expression in rice roots. *New Phytologist* 197: 791–804.